Environ. Sci. Technol. 2000, 34, 1150–1155

Reactive Uptake of Trace Metals in the Hyporheic Zone of a Mining-Contaminated Stream, Pinal Creek, Arizona

CHRISTOPHER C. FULLER*,† AND JUDSON W. HARVEY‡

U.S. Geological Survey, Menlo Park, California, and U.S. Geological Survey, Reston, Virginia

Significant uptake of dissolved metals occurred by interaction of groundwater and surface water with hyporheic-zone sediments during transport in Pinal Creek, AZ. The extent of trace metal uptake was calculated by mass balance measurements made directly within the hyporheic zone. A conservative solute tracer injected into the stream was used to quantify hydrologic exchange with the stream and groundwater. Fractional reactive uptake of dissolved metals entering the hyporheic zone was determined at 29 sites and averaged 52 ± 25, 27 ± 19, and 36 ± 24% for Co, Ni, and Zn, compared with Mn uptake of 22 ± 19%. First-order rate constants (λ_h) of metal uptake in the hyporheic zone were determined at seven sites using the exchange rate of water derived from tracer arrival in the streambed. Reaction-time constants ($1/\lambda_h$) averaged 0.41, 0.84, and 0.38 h for Co, Ni, and Zn, respectively, and 1.3 h for Mn. In laboratory experiments with streambed sediments, metal uptake increased with preexisting Mn oxide concentration, supporting our interpretation that Mn oxides in the hyporheic zone enhance trace metal uptake. Reach-scale mass-balance calculations that include groundwater metal inputs indicated that decreases in metal loads ranged from 12 to 68% over the 7-km perennial reach depending on the metal. The decreases in metal loads are attributed to uptake of trace metals by Mn oxides in the hyporheic zone that is enhanced because of ongoing Mn oxide formation. Analysis of dissolved-metal streambed profiles and conservative solute tracers provide a valuable tool for quantifying metal uptake or release in the hyporheic zone of contaminated streams.

Introduction

Assessing the ability of a stream to attenuate contaminant loads is critical to understanding the fate of mining-related metal contaminants. The extent of natural attenuation in a stream is dependent on the accessibility of reactive solutes to zones favorable for chemical reactions. Exchange of surface water through the streambed can enhance metal attenuation by transporting metals into zones where removal processes are more favorable (*1*–*3*). The portion of a streambed containing a mixture of surface-water and groundwater is referred to as the hyporheic zone, which is defined as having a component of at least 10% surface water (*4*). Flow of surface water in the hyporheic zone increases the effective reactive site density per volume of surface water by providing contact of dissolved metals with potential reaction or sorption sites within the streambed. At Pinal Creek, AZ, we previously determined that microbially enhanced oxidation of dissolved Mn in the hyporheic zone resulted in a net decrease of 20% in the Mn load flowing out of the drainage basin (*5*).

The focus of the present study was to evaluate the role of the hyporheic zone for uptake of dissolved Co, Ni, and Zn. Because enhanced oxidation of Mn in the hyporheic zone results in ongoing formation of Mn oxide coatings on sediments (*5*), we hypothesize that manganese oxidation continuously forms new sorption sites that should enhance removal of trace metals. This hypothesis is based on the affinity of metals for sorption or coprecipitation by Mn oxides (*6*–*11*). The uptake of dissolved metals in the hyporheic zone was determined by modeling dissolved metal profiles in the streambed using methods developed by our previous study (*5*). A solute tracer was introduced into the hyporheic zone by in-stream injection to quantify surface-water exchange with the hyporheic zone and to determine the extent and rate of metal uptake. Laboratory measurements of metal adsorption by streambed sediments were conducted to determine if Mn oxides enhanced Co, Ni, and Zn uptake.

Site Description. Pinal Creek is a sand and gravel bed stream with a 1% average slope (*5*). Perennial flow results from constriction of an alluvial aquifer by underlying bedrock in the Pinal Creek basin. Mining operations have generated a plume of acidic groundwater (pH < 4, 18 mM Fe, 1.5 mM Cu) in the alluvial aquifer upgradient of the perennial stream. Reaction of acidic groundwater with aquifer sediments has formed a plume of neutralized (pH 5.5–6.5), contaminated groundwater with elevated dissolved Mn, Co, Ni, and Zn of up to 1.5 mM, 20, 25, and 25 μM, respectively (*12*). Water chemistry of Pinal Creek is dominated by discharge of this neutralized, contaminated groundwater (Figure 1), which contributes about 50% of the base-flow discharge at Inspiration Dam (*13*), where Pinal Creek exits the alluvial basin. Streamwater chemistry is characterized by high dissolved solids (e.g. SO_4 23 mM; Ca 13 mM) and elevated dissolved Mn, Co, Ni, and Zn. Stream and groundwater Mn and Ni increased from background levels from 1980 to 1990 with little subsequent change (*14*). Co and Zn increased by about a factor of 15 in shallow groundwater since 1990. Crusts of Mn-oxide cemented sediments cover the streambed in some reaches of the stream (*13*).

Methods

Vertical profiles of dissolved metals in the streambed were measured at 2 sites in June 1994, 3 sites in June 1995, and 24 sites in May 1997 (Figure 1). The hyporheic-zone sampling sites were located in areas without Mn-oxide cemented streambed. The data presented here expands the previous analysis presented in Harvey and Fuller (*5*) by including the 1997 data set and by focusing on the fate of trace metals.

Dissolved metal and tracer samples were collected at close depth intervals in the streambed (2.5-cm) over a 10- or 15-cm depth using a minidrivepoint (MINIPOINT) sampler (*15*, *5*). This device consists of six 3-mm diameter stainless steel piezometers in a circular array installed into the streambed about an hour before sampling. All depths were sampled simultaneously by multihead peristaltic pump at 4 mL per min. This rate did not disturb the vertical profile of a conservative tracer that had reached plateau concentration (*15*). Samples for dissolved cations and field water quality

* Corresponding author phone: (650)329-4479; fax: (650)329-4545; e-mail: ccfuller@usgs.gov.
† U.S. Geological Survey, Menlo Park, CA.
‡ U.S. Geological Survey, Reston, VA.

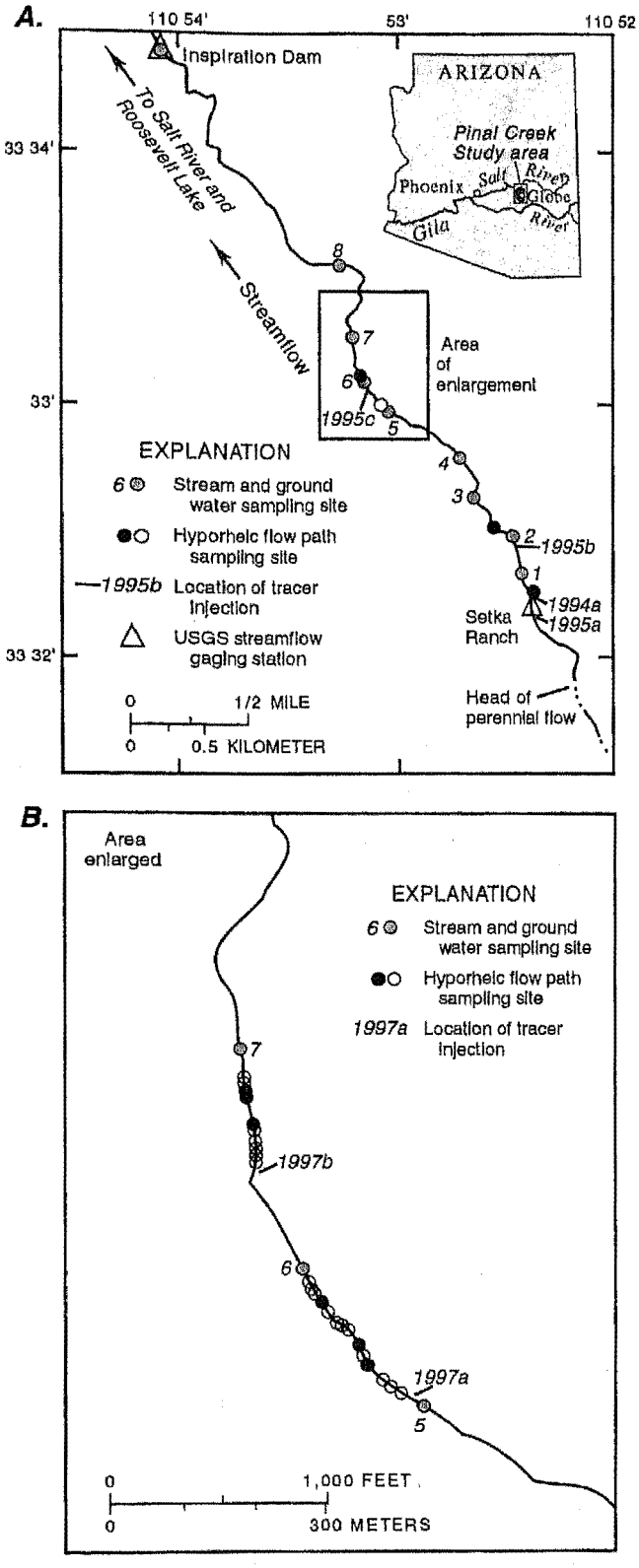

FIGURE 1. Site map showing location of (A) the perennial streamflow of Pinal Creek and the 2.8-km study reach with surface-, ground-, and hyporheic-zone sites sampled in 1994 and 1995 and (B) subreach sampled in 1997. Open circles depict hyporheic-zone sites sampled for tracer and dissolved metals after tracer had reached plateau. Solid circles depict hyporheic-zone sites that also were sampled for tracer arrival time.

parameters (pH, DO, and alkalinity) were collected after tracer samples. Water samples also were collected from 9.5-mm diameter stainless steel drive point piezometers inserted 30–200 centimeters (cm) into the streambed at each site. Surface-water samples were collected by dipping into the stream at each MINIPOINT travel time site and at subreach endpoints depicted by numbered points in Figure 1.

All dissolved metal samples were filtered through 0.45-μm pore-size filters that are effective because the colloidal metal fraction is not significant in Pinal Creek (*16*). Release of metals from stainless steel piezometers or sorption by sampling devices was negligible in laboratory tests. Dissolved cation and Si concentrations were determined by ICP-OES (inductively coupled plasma-optical emission spectroscopy). Method detection limits (*17*) were 0.4, 1.1, 1.6, and 0.3 μM for Co, Mn, Ni, and Zn, respectively. Coefficient of variation of ICP-OES analyses averaged 3.2, 1.9, 3.4, 2.4, and 2.3% for Co, Mn, Ni, Zn, and Si, respectively. The variability of replicate surface-water samples was similar to these coefficients of variation.

The fraction of surface water in the hyporheic zone was determined from the tracer concentration at each depth relative to surface-water tracer concentration at that site. Groundwater inflow concentrations were defined by drive-point samples from below the depth of tracer penetration. The in-stream conservative tracer injections and modeling of their results are described in Harvey and Fuller (*5*). Dissolved bromide (Br) was injected upstream of MINIPOINT sites at a constant rate for between 3 and 4 h to attain a steady-state streamwater Br of 40–65 μM. Travel time for tracer arrival in hyporheic zones was measured at all sites in 1994 and 1995 and at six sites in 1997. This was accomplished by continuously sampling a MINIPOINT sampler for 3 h after commencement of tracer injection. Samples were collected at 3 min intervals over the first 20 min followed by 5-min intervals through 1 h with 10-min intervals to 3 h after the start of the injection. Metal samples were collected after Br concentrations had plateaued, typically 2–3 h after the tracer injection began. Bromide concentrations were measured by ion chromatography with a detection limit of 0.03 μM and coefficient of variation of 2.5%.

Streambed cores of up to 30-cm depth were collected at each site where Br travel time was measured. Cores were sectioned at 3- or 4-cm intervals, air-dried, and sieved to remove the >1 mm size fraction. Sediment metal concentrations were determined by partial extraction with 0.1 M NH_2-OH·HCl in 0.05-M nitric acid for 1 h (HH). This method modified from ref *18* was effective at dissolving Mn coatings from sediments. Use of longer extraction times or higher concentration or temperature did not result in an increase in Mn concentration. HH extracts were analyzed by ICP-OES.

Metal uptake by streambed sediments also was determined in laboratory batch experiments. Sediments were collected at four sites along the perennial reach from the upper 2 cm of the streambed. Particles > 1 mm were removed by wet sieving because this size fraction was difficult to sample representatively for the amounts used in each batch experiment. A second sample from each site was mixed with an equal volume of streamwater containing sodium azide (15 mM) to test the effect of microbial Mn oxidation, which enhances Mn uptake (5). Wet sediments were added to an artificial groundwater of similar major ion composition to Pinal Creek in polycarbonate centrifuge tubes. A sediment concentration of 160 g/L was used. The pH was controlled at 7 ± 0.1 units by imposing a 1% CO_2 in air mixture for the gas phase. Metal uptake was initiated by addition of filtered, neutralized groundwater at pH 7 with the resulting initial dissolved metal concentrations that are similar to surface water in the study reach. At each time point, supernatant from a pair of tubes was sampled after centrifugation. Metal uptake was calculated from the change in dissolved metal concentration determined by ICP-OES. Sediment metal

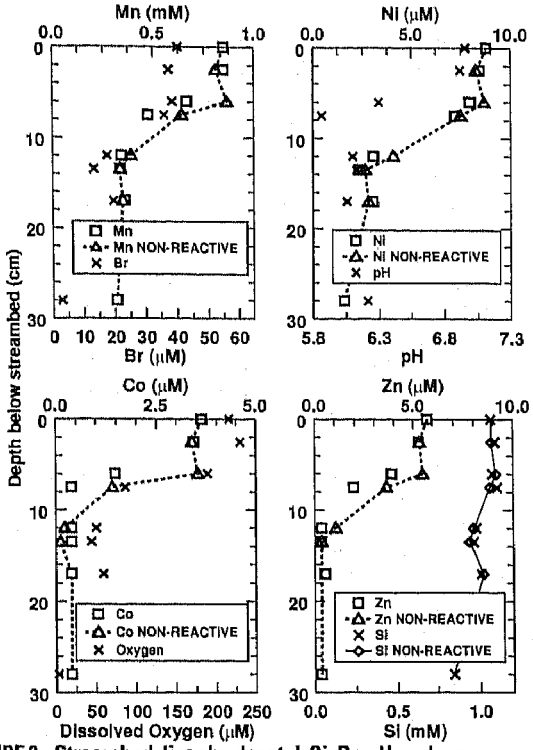

FIGURE 2. Streambed dissolved metal, Si, Br, pH, and oxygen profiles at a site with a hyporheic zone of over 17-cm depth. Calculated nonreactive metal and Si concentrations also are plotted. Surface water concentrations are shown at 0 cm. Values at 28-cm represent average concentration in groundwater. Significant uptake was calculated at 6- and 7.5-cm for all metals and at 12 cm for Mn, Ni, and Zn.

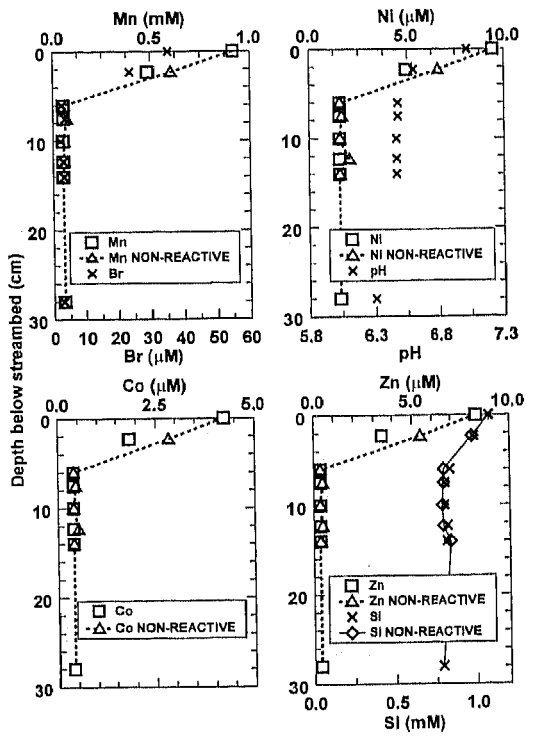

FIGURE 3. Streambed dissolved metal, Br, and pH profiles at a site with a 3-cm hyporheic zone. Calculated nonreactive metal concentrations also are plotted. Surface water concentrations are shown at 0 cm. Values at 28-cm represent average concentration in groundwater. Significant uptake was calculated at 3-cm for all metals.

concentrations also were measured on these sediments using HH extraction. Desorption of preexisting metals on the sediments was tested in batch experiments without added metals.

Results and Discussion

Dissolved Mn, Co, Ni, and Zn in the streambed decreased in concentration with depth below surface water (Figures 2 and 3). In the upstream end of the reach, dissolved Mn and Ni increased with depth because of higher concentrations in the inflowing shallow groundwater. The penetration of Br tracer into the streambed ranged from less than 2.5 cm to over 15 cm among the 29 sites sampled. Based on Br concentration, 26 sites had a surface-water component of 10% or greater at depths of 2.5 cm or deeper and are therefore considered as hyporheic zone sites (*4*). Travel time for tracer arrival in the subsurface ranged from <2 to 80 min among the nine sites sampled for tracer arrival. Travel time was defined as the elapsed time for Br to reach 50% of plateau at any depth relative to the next shallower depth (*5*).

Streamwater dissolved metal concentrations decreased 30% or more downstream along the 2.8-km study reach (Figure 4). Surface-water pH increased from about 6.5 to 7.5 downstream over the study reach because of CO_2 outgassing (*19*). Mn and Ni concentrations in groundwater were equal to or greater than in surface water over the first 0.6 km of the study reach. Groundwater Mn decreased to background by 1.2 km; Ni decreased to below detection limit by 1 km; Co and Zn were above background in groundwater only at the upstream sites. Equilibrium speciation calculations indicated dissolved Co, Ni, and Zn at all sites were below saturation with respect to solid phases such as carbonate or hydroxides. Free ion and sulfate complexes dominated dissolved metal speciation.

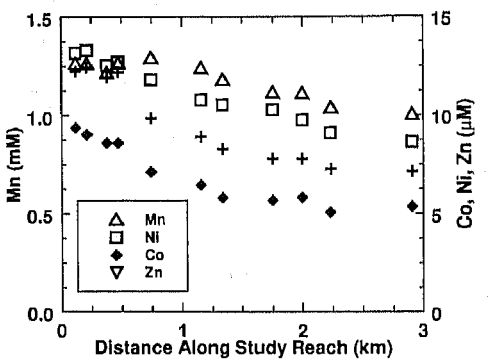

FIGURE 4. Surface-water dissolved metal concentrations in June 1995 over the 2.8-km study reach.

Hyporheic-Zone Profile Analysis. We calculated whether metal uptake or release occurred in the hyporheic zone using a steady-state transport model developed by Harvey and Fuller (*5*)

$$\hat{C}_h^{i+1} = C_h^i + \beta^{i+1/2}(C_L - C_h^i) - \lambda_h^{i+1/2}\tau_h^{i+1/2}(C_h^i + C_h^{i+1})/2 \quad (1)$$

where C_h is the metal concentration in the hyporheic zone, C_L is groundwater metal concentration, τ_h is the travel time of tracer, β is the fraction of groundwater in a depth increment, and λ_h is the first-order metal uptake rate constant in the hyporheic zone. The circumflex indicates a calculated concentration. The superscript i refers to a specific sampling depth, $i+1$ refers to the next deeper depth, and $i+1/2$ to the average value for the interval between sampling depths.

The mixing of surface and groundwater within the hyporheic zone was calculated from Br tracer data. In eq 1, the fraction of groundwater input at any depth, $\beta^{i+1/2}$, was

TABLE 1. Fractional Percent Metal Uptake, f_M, for All Hyporheic Zone Sites and Depths with Significant Metal Uptake

	Mn	Co	Ni	Zn
av	22	52	27	36
number of values	39	39	32	41
SD	19	25	19	24
maximum	94	100	74	92
minimum	5	8	7	7

determined from measurements of the Br tracer after concentrations had reached plateau at all depths

$$\beta^{i+1/2} = \frac{\mathrm{Br}_h^{i+1} - \mathrm{Br}_h^{i}}{\mathrm{Br}_L - \mathrm{Br}_h^{i}} \quad (2)$$

where Br is the tracer concentration for the depths denoted by subscripts and superscripts used in eq 1. $\beta^{i+1/2}$ was assumed to equal 1 at depths where Br concentration was equal to or less than Br background.

We used eq 1 in two ways. First, a nonreactive metal profile was calculated by setting $\lambda_h = 0$ in eq 1 and solving for $\hat{C}_h^{i+1}$ assuming conservative transport (Figures 2 and 3). Second, metal-uptake rate constants for each depth interval were calculated by solving for λ_h, the first-order rate constant for metal uptake. The difference between C_h^{i+1} and $\hat{C}_h^{i+1}$ was assumed to represent metal uptake by sediments if $\hat{C}_h^{i+1}$ was greater than C_h^{i+1}, or release if C_h^{i+1} was greater than $\hat{C}_h^{i+1}$. Metal uptake was expressed as a percentage of the difference between the calculated concentration without reaction and the measured concentration

$$f_M = \frac{C_h^{i+1} - \hat{C}_h^{i+1}}{\hat{C}_h^{i+1}} \times 100 \quad (3)$$

where f_M is the percent metal uptake. In some cases C_L or C_h^{i+1} were below the analytical detection limit. In those cases the detection limit was used for calculation.

The total uncertainty in the calculated metal concentration, $\hat{C}_h^{i+1}$, σ_C, was estimated by propagating the coefficients of variation for metal concentrations and σ_β through eq 1. The uncertainty in C_h^{i+1} was estimated from the average coefficient of variation for metal analyses by ICP-OES. The uncertainty in $\beta^{i+1/2}$, σ_β, was estimated from the average coefficient of variation of Br measurements propagated through eq 2. Uptake or release was termed insignificant if $|C_h^{i+1} - \hat{C}_h^{i+1}|$ was less than the sum of σ_C and the uncertainty in C_h^{i+1}. Depths with an insignificant difference were not considered further.

Hyporheic-Zone Metal Uptake. Significant metal uptake was observed at 75–96% of hyporheic zone sites depending on the metal. The extent of reactive uptake is illustrated by comparison of the calculated, nonreactive concentrations to the measured concentrations in two hyporheic zone profiles (Figures 2 and 3). Dissolved Si was used to test the hyporheic-zone calculations assuming Si is a conservative solute. No significant difference between C_h^{i+1} and $\hat{C}_h^{i+1}$ was observed for Si at more than 90% of hyporheic zone sites or intervals. This result supports the reliability of our calculations of surface- and groundwater mixing within the hyporheic zone.

A wide range in the percent uptake was found for all metals (Table 1). The Co and Zn average percent uptake were both greater than Mn uptake, with Ni uptake similar to Mn uptake. The average f_{Mn} for this expanded data set is significantly greater than the average f_{Mn} reported in our previous study

TABLE 2. Metal Uptake Rate Constant, λ_h, and Uptake Time Constant ($1/\lambda_h$) in Hours for Hyporheic Zone and for Laboratory Uptake Experiments[a]

	Mn	Co	Ni	Zn
av λ_h (min^{-1})	0.013	0.041	0.020	0.058
number of values	11	9	5	9
SD	0.014	0.035	0.022	0.037
av time constant (h)	1.3	0.41	0.84	0.38
laboratory time constant range (h)	2–4	0.2–0.9	0.5–1.6	0.2–0.6

[a] Laboratory uptake time constants were scaled to the sediment concentration of the streambed.

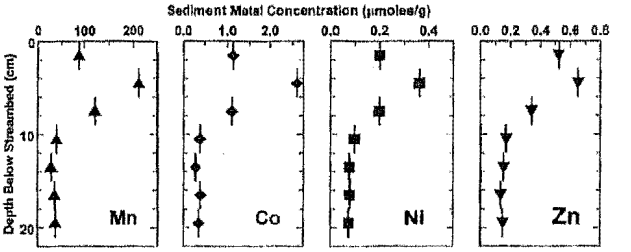

FIGURE 5. Metal concentration profiles from extracted streambed sediment at the site with the 17-cm hyporheic zone shown in Figure 2. Elevated sediment metal concentrations are observed at depths where dissolved metal uptake is calculated.

(5) from the 1994 and 1995 data alone. Because the oxidation rate of Mn by Pinal Creek sediments increases with increasing pH (20), this difference may be due to the higher surface-water pH of the reach sampled in 1997. The 1997 sites are located in the lower end of the 2.8-km study reach along a 0.5-km reach downstream of all significant groundwater metal inputs, where streamwater pH ranged from 7.0 to 7.2. Trace metal uptake typically increased with increasing Mn uptake. However, only Co and Mn uptake are significantly correlated ($p < 0.05$). Metal-uptake rate constants, λ_h, varied widely among the seven sites where they could be estimated (Table 2). However, λ_h for Co, Ni, and Zn was always greater than λ_h for Mn at a site.

Sediment Metal Concentrations. Concentrations of Co, Ni, Zn, and Mn in bed sediments typically were elevated by a factor of 2 or more in the active hyporheic zone compared to deeper sediments (Figure 5). The depth range of elevated sediment metal concentrations coincides with the zone where reactive metal uptake was calculated. The presence of elevated concentrations of trace metals and Mn in the hyporheic-zone sediments is consistent with metal uptake occurring in the streambed.

For all metals, about half of the hyporheic-zone sites had no significant difference between measured and nonreactive dissolved concentrations at the 2.5-cm depth, but most of these sites had measurable uptake at the deeper depths (e.g. Figure 2). The elevated sediment metal concentrations in the 0–3 cm interval at this site indicate uptake has occurred (Figure 5). Because of the short residence time of water at 2.5-cm (<2 min) relative to the average λ_h, the change in metal concentration cannot be distinguished from the metal concentration of water entering this depth.

Laboratory Metal Uptake Experiments. Uptake of Co, Ni, and Zn by streambed sediments in batch experiments increased with increasing concentration of preexisting Mn oxides defined by HH extraction (Figure 6). Because metal uptake was measured under identical experimental conditions (pH, sediment-to-water ratio, and initial metal concentration), the observed increase in metal uptake with Mn oxide concentration indicates that Mn oxides are an important sorbent phase in Pinal Creek sediments. Exclusion

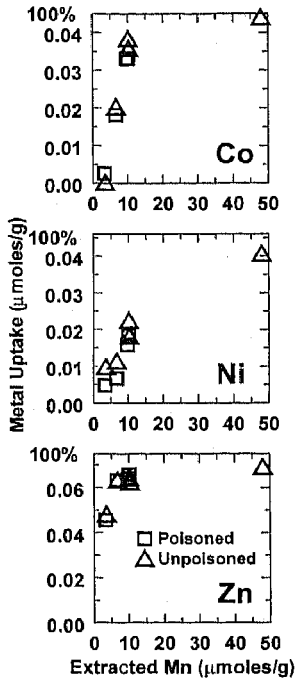

FIGURE 6. Co, Ni, and Zn uptake by streambed sediments increase with preexisting sediment Mn oxide concentration. Experiments were conducted using a sediment concentration of 160 g per L, and initial dissolved Co, Ni, and Zn of 7.2, 7.5, and 9.2 μM, respectively. Complete uptake of the added metal is denoted as 100% on the *y*-axis.

of microbial Mn oxidation by addition of sodium azide (*5*) had little effect on trace-metal sorption, probably because preexisting Mn oxide sites were available during the course of these experiments. Sediment concentrations of Co, Ni, and Zn prior to uptake experiments ranged from equal to five times the amount of uptake measured in the batch experiments. However, desorption of the preexisting metals was not detected in the batch experiments with no added dissolved metals. The uptake of metals observed suggests that these sediments had additional sorption capacity for Co, Ni, and Zn.

Uptake of Co, Ni, and Zn by streambed sediments occurs rapidly over the first 10 h followed by a slower approach to equilibrium through 4 days. Apparent first-order rate constants were calculated for uptake over the first 10 h during which more than 75% of the uptake occurred. Rate constants were scaled linearly to account for the higher sediment concentration (2520 g/L) in the streambed compared to the batch experiments (160 g/L). Streambed sediment concentration was estimated using a measured porosity of 0.3 and a sediment density of 2.7 g/cm^3 and assuming uptake occurs primarily on the <1 mm fraction, which is about 40% of sediment mass (*5*). Scaled time constants for metal uptake (Table 2) have a similar range to the time constants for metal uptake calculated from hyporheic zone profiles. The agreement between field and laboratory time constants supports the validity of our field estimates of metal uptake in the hyporheic zone that separate hyporheic exchange from metal uptake. Although metal uptake rates can vary strongly with pH, the experimental pH 7 was chosen because it is near the middle of the pH range of the study reach. The pH-dependence of metal uptake by Pinal Creek sediments is part of our ongoing investigation.

Metal Uptake Processes. The observed uptake of trace metals in the hyporheic zone is postulated to result from reaction or surface complexation with Mn oxide surfaces concurrently forming on streambed sediments. Mn precipitation forms thick coatings on sediment grains primarily as oxides (pyrolusite, rancieite, todorokite) with some carbonates present (rhodochrosite, kutnahortite) (*21*, *22*). The absence of dissolved iron and low colloidal Fe concentrations suggest that Fe oxides have a minor role in trace-metal uptake. In addition, the ongoing formation of Mn coatings probably has covered any preexisting Fe-oxide surfaces.

TABLE 3. Mass Balance of Dissolved Metal Loads for 5.3-km Reach[a]

	Mn	Co	Ni	Zn
1994				
upstream input	159	0.27	1.37	0.36
groundwater input over reach	67	0.05	0.27	0.03
total input	226	0.32	1.64	0.38
downstream load	187	0.10	1.44	0.21
load decrease	39	0.22	0.20	0.17
% decrease	17	68	12	45
1995				
upstream input	155	1.16	1.62	1.51
groundwater input over reach	111	0.11	0.48	0.08
total input	266	1.27	2.10	1.59
downstream load	196	0.80	1.65	0.98
load decrease	70	0.47	0.45	0.61
% decrease	26	37	22	38

[a] Loads in millimoles per second.

The dependence of metal uptake on sediment Mn oxide concentration in laboratory experiments indicates that Mn oxide is an important sorbent for trace metals in Pinal Creek sediments. The role of Mn oxides as a metal absorbent is further evident from X-ray absorption spectroscopic data, which suggests that Zn on metal-contaminated sediments is likely coordinated by Mn(III) and Mn(IV) octahedra (*23*). These data are consistent both with adsorption of Zn as a surface complex by Mn oxides and with substitution of Zn into a Mn oxide phase. Elemental mapping of sediment grains using laser-ablation ICP-MS indicated trace metals are associated with Mn oxide coatings, probably resulting from cation substitution into interlayers of birnessite or in tunnel structures of other Mn oxides and with Mn carbonates (*22*). These findings coupled with the elevated concentrations of both Mn and trace metals in hyporheic-zone sediments suggest that uptake of trace metals largely occurs by sorption to Mn oxides. Because metal uptake was calculated at most sites, we propose that the ongoing Mn oxide formation in the hyporheic zone (*5*) enhances metal uptake compared to streams where formation of sorbent phase is not occurring.

Effect of Hyporheic Zone Metal Uptake on Transport. Previously, we determined that enhanced Mn oxidation in the hyporheic zone accounts for the net uptake of 20% of Mn over the 5.3-km perennial reach to Inspiration Dam (*5*). The extent of trace-metal uptake was determined from the difference between the metal load at Inspiration Dam and the sum of the load at the upstream end of the 2.8-km reach and groundwater metal inputs to the stream. Groundwater metal inputs were calculated from the groundwater inflow to each subreach between surface water sampling sites (Figure 1) times the average of the groundwater metal concentration at these sites. Groundwater inflow was determined from the change in stream discharge over each subreach using the surface-water Br tracer for dilution gaging (*5*). Groundwater metal input downstream of the 2.8-km reach was considered negligible. Mass balance calculations for the 1994 and 1995 data indicate net attenuation of trace metals over the perennial reach ranging from 12 to 68% (Table 3). We attribute these significant decreases in trace-metal loads to enhanced Mn oxidation and subsequent metal uptake in the hyporheic zone.

On a basin scale, attenuation of metals is limited by the exchange rate of surface water into the streambed and the dimensions of the hyporheic zone, which controls the availability of sorption sites. A wide variability in the extent of metal uptake was observed among sites (Table 1), some of which were located within 10 m. Factors that contribute to the observed variability in f_M likely include Mn-oxide content, population of Mn oxidizing bacteria, residence time of water in the hyporheic zone, and pH. Investigation of factors affecting hyporheic-zone metal uptake is a topic of our ongoing investigation.

Our findings demonstrate the importance of Co, Ni, and Zn uptake by Mn oxides forming in the shallow hyporheic zone (<15 cm) of a contaminated stream. Enhanced Mn oxidation in the hyporheic zone also probably affects metal and metalloid transport in other streams with elevated Mn. For example, high Mn concentrations are reported in streams draining coal-mining areas (*24*). A related problem is Mn-oxide dissolution and subsequent Mn oxidation farther along the flow path observed during infiltration of contaminated river water into an alluvial aquifer (*25*). In that study, uptake of dissolved Zn may have resulted from adsorption to Mn oxides. Further investigation in rivers and streams is warranted using our approach of in-situ hyporheic-zone measurements to quantify metal uptake or release. We recommend this approach be used in conjunction with reach-scale tracer studies to improve the understanding of chemical and hydrologic processes that control the fate and transport of metals (*5, 26*) and metalloids (*27*) in streams.

Acknowledgments

This study was funded in part by the USGS Toxics Substances Hydrology Program. Fieldwork assistance by C. Angeroth, J. Brown, J. Choi, M. Conklin, T. Corely, S. Ferguson, H. Flinchbaugh, D. Weinig, D. Graham, J. Marble, B. Wagner, and G. Zellweger is gratefully acknowledged. We thank J. Choi and Y. Hunter for assistance in laboratory analyses. J. Kuwabara, K. Smith, and three anonymous reviewers provided helpful comments that improved the manuscript.

Literature Cited

(1) Bencala, K. E.; Kennedy, V. C.; Zellweger, G. W.; Jackman, A. P.; Avanzino, R. J. *Water Resour. Res.* **1984**, *20*, 1797–1803.
(2) Kimball, B. A.; Broshears, R. E.; Bencala, K. E.; McKnight, D. M. *Environ. Sci. Technol.* **1994**, *28*, 2065–2073.
(3) Benner, S. G.; Smart, E. W.; Moore, J. N. *Environ. Sci. Technol.* **1995**, *29*, 1789–1795.
(4) Triska, F. J.; Duff, J. H.; Avanzino, R. J. *Hydrobiologia* **1993**, *251*, 167–184.
(5) Harvey, J. W.; Fuller, C. C. *Water Resour. Res.* **1998**, 34, 623–636.
(6) Balistrieri, L. S.; Murray, J. W. *Geochim. Cosmochim. Acta* **1986**, 50, 2235–2243.
(7) Catts, J. G.; Langmuir, D. L. *Appl. Geochem.* **1986**, *1*, 255–264.
(8) Tessier, A.; Fortin, D.; Belzile, N.; DeVitre, R. R.; Leppard, G. G. *Geochim. Cosmochim. Acta* **1996**, *60*, 387–404.
(9) Hem, J. D.; Roberson, C.E.; Lind, C. J. *Geochim. Cosmochim. Acta* **1985**, *49*, 801–810.
(10) Hem, J. D.; Roberson, C.E.; Lind, C. J. *Geochim. Cosmochim. Acta* **1987**, *51*, 1539–1547.
(11) Hem, J. D.; Roberson, C.E.; Lind, C. J. *Geochim. Cosmochim. Acta* **1989**, *53*, 2811–2822.
(12) Stollenwerk, K. G. *Appl. Geochem.* **1994**, *9*, 353–369.
(13) Eychaner, J. H. In *USGS Toxic Substances Hydrology Program Proceedings*; WRIR 91-4034; USGS: 1991; pp 481–485.
(14) Brown, J. G.; Harvey, J. W. In *USGS Toxic Substances Hydrology Program Proceedings*; WRIR **94**-4014; USGS: 1996; pp 1035–1042.
(15) Duff, J. H.; Murphy, F.; Fuller, C. C.; Triska, F. J.; Harvey, J. W.; Jackman, A. P. *Limnol. Oceanog.* **1998**, *43*, 1378–1383.
(16) Harvey, J. W.; Fuller, C. C. In *USGS Toxic Substances Hydrology Program Proceedings*; WRIR 94-4014; USGS: 1996; pp 1073–1080.
(17) Glaser, J. A.; Foerst, D. L.; McKee, G. D.; Quave, S. A.; Budde, W. L. *Environ. Sci. Technol.* **1981**, *15*, 1426–1435.
(18) Chou, T. T. *J. Geochem. Explor.* **1984**, *20*, 101–135.
(19) Choi, J.; Hulseapple, S.; Conklin, M. H.; Harvey, J. W. *J. Hydrol.* **1998**, *209*, 297–310.
(20) Marble, J. C. M.S. Thesis, University of Arizona, 1998.
(21) Lind, C. J.; Hem, J. D. *Appl. Geochem.* **1993**, *8*, 67–80.
(22) Geiger, K. E. M.S. Thesis, Arizona State University, 1999.
(23) O'Day, P. A.; Geiger, K. E.; Fuller, C. C. *Water Rock Interaction- - Proceedings of the 9th International Symposium*; WRI-9; Arehart, G. B., Hulston, J. R., Eds.; 1998; pp 993–996.
(24) Tarutis, W. J.; Unz, R. F.; Brooks, R. P. *Appl. Geochem.* **1992**, *7*, 77–86.
(25) Bourg, A. C. M.; Bertin, C. *Environ. Sci. Technol.* **1993**, *27*, 661–666.
(26) Runkel, R. L.; McKnight, D. M.; Bencala, K. E.; Chapra, S. C. *Water Resour. Res.* **1996**, *32*, 419–430.
(27) Nagorski, S. A.; Moore, J. N. *Water Resour. Res.* **1999**, *34*, 3441–3450.

Received for review June 27, 1999. Revised manuscript received December 8, 1999. Accepted December 29, 1999.

ES990714D